Acta Crystallographica Section D
Biological Crystallography
ISSN 0907-4449

Structural studies of hydrogen bonds in the high-affinity streptavidin–biotin complex: mutations of amino acids interacting with the ureido oxygen of biotin

Isolde Le Trong,[a]† Stefanie Freitag,[a,b]† Lisa A. Klumb,[b] Vano Chu,[b] Patrick S. Stayton[b] and Ronald E. Stenkamp[a]*

[a]Department of Biological Structure and Biomolecular Structure Center, University of Washington, Box 357420, Seattle, Washington 98195-7420, USA, and [b]Department of Bioengineering, University of Washington, Box 352125, Seattle, Washington 98195-2125, USA

† S. Freitag and I. Le Trong should be considered co-first authors.

Correspondence e-mail: stenkamp@u.washington.edu

Received 20 March 2003
Accepted 30 June 2003

PDB References: streptavidin mutant N23A, 1n4j, r1n4jsf; biotin complex of N23A, 1n43, r1n43sf; mutant N23E, 1n7y, r1n7ysf; mutant S27A, 1n9y, r1n9ysf; biotin complex of S27A, 1n9m, r1n9msf; mutant Y43A, 1nbx, r1nbxsf; 2-iminobiotin complex of Y43A, 1nc9, r1nc9sf; mutant Y43F, 1swu, r1swusf; biotin complex of Y43F, 1ndj, r1ndjsf.

An elaborate hydrogen-bonding network contributes to the tight binding of biotin to streptavidin. The specific energetic contributions of hydrogen bonds to the biotin ureido oxygen have previously been investigated by mapping the equilibrium and activation thermodynamic signatures of N23A, N23E, S27A, Y43A and Y43F site-directed mutants [Klumb *et al.* (1998), *Biochemistry*, **37**, 7657–7663]. The crystal structures of these variants in the unbound and biotin-bound states provide structural insight into the energetic alterations and are described here. High (1.5–2.2 Å) to atomic resolution (1.14 Å) structures were obtained and structural models were refined to R values ranging from 0.12 to 0.20. The overall folding of streptavidin as described previously has not changed in any of the mutant structures. Major deviations such as side-chain shifts of residues in the binding site are observed only for the N23A and Y43A mutations. In none of the mutants is a systematic shift of biotin observed when one of the hydrogen-bonding partners to the ureido oxygen of biotin is removed. Recent thermodynamic studies report increases of $\Delta\Delta G^{\circ}$ of 5.0–14.6 kJ mol^{-1} for these mutants with respect to the wild-type protein. The decreasing stabilities of the complexes of the mutants are discussed in terms of their structures.

1. Introduction

Streptavidin displays a very high affinity for biotin ($K_d \simeq 10^{-13}$ M; Green, 1963). This exceptional interaction makes streptavidin–biotin a good model system for the study of protein–ligand energetics. Deciphering the underlying structure–function relationships will provide basic insight into protein–ligand interactions and could be useful in biotechnological applications and structure-based drug design. Previously, we have reported investigations of the hydrophobic contributions (Chilkoti & Stayton, 1995; Chilkoti *et al.*, 1995; Freitag *et al.*, 1998) and also of the biotin-binding loop (Freitag *et al.*, 1997; Chu *et al.*, 1998) in the streptavidin–biotin system. Likewise, we have investigated the effects of mutations altering the hydrogen bonds to the ureido N atoms of biotin (Freitag *et al.*, 1999; Hyre *et al.*, 2000). Here, we report crystallographic analyses of mutations of the three streptavidin hydrogen-bonding residues, Asn23, Ser27 and Tyr43 (Klumb *et al.*, 1998), that interact with biotin through hydrogen bonds to the ureido O atom of the ligand.

The hydrogen-bonding network involving streptavidin and the ureido group of biotin is shown in Fig. 1. Weber *et al.* (1989) suggested that stabilization of an oxyanion resonance form of the biotin ureido oxygen could result in exceptionally strong hydrogen bonds between the ligand and the protein. An sp^3-hybridized ureido O atom would be able to accept the three observed hydrogen bonds from Asn23, Ser27 and Tyr43.

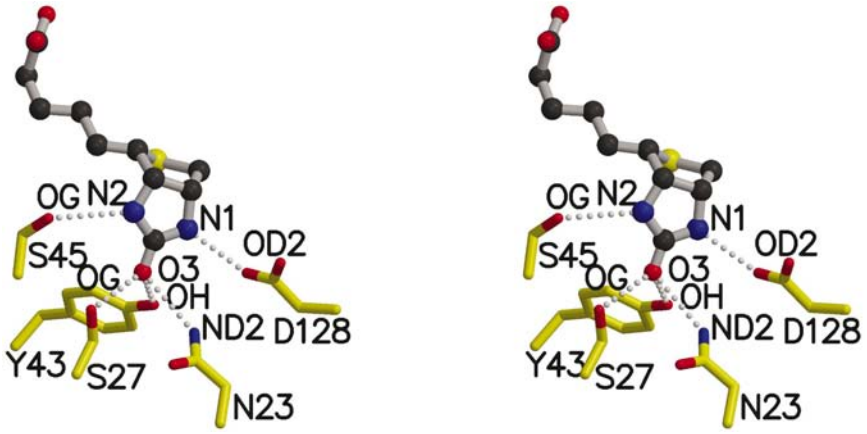

Figure 1
Stereoview showing the hydrogen bonds between streptavidin and the ureido group of biotin. Figure drawn with *MOLSCRIPT* (Kraulis, 1991) and *Raster3D* (Merritt & Bacon, 1997).

The distances of these interactions range from 2.6 to 3.1 Å in wild-type streptavidin. Systematic mutations of these three residues to alter and remove the hydrogen-bonding interactions have been carried out and the binding constants (K_d) of the mutants are reduced by between sevenfold and 282-fold (Klumb *et al.*, 1998). The effects of those mutations on the three-dimensional structures of the proteins and their ligand complexes were determined to correlate structural and functional changes.

2. Experimental

2.1. Protein characterization

Design and construction of the recombinant gene and site-directed mutagenesis, expression, isolation, purification and characterization of the streptavidin mutants have been described previously (Klumb *et al.*, 1998). The determination of binding free-energy alterations with a new developed assay, isothermal titration calorimetry (ITC) for binding enthalpies, streptavidin–biotin dissociation kinetics using radioactive-labeled biotin and activation thermodynamic parameters determined by transition-state analysis are also reported there.

2.2. Crystallization

Solutions of the proteins at concentrations of 20–30 mg ml^{-1} in water were used for hanging-drop or sitting-drop vapor-diffusion crystallization experiments. Crystals were obtained from 50% MPD (2-methyl-2,4-pentanediol) solutions, except for the N23A mutant and the biotin complex of Y43F. N23A crystals were obtained with a 10% PEG 4000, 0.1 *M* phosphate buffer pH 6.2 solution. The Y43F–biotin complex crystallized from 16% PEG 4000, 0.1 *M* HEPES buffer pH 7.5. For co-crystallization with biotin or 2-iminobiotin, the protein solutions were incubated overnight with a 2.5 molar excess of the ligand. The unit-cell parameters for all crystals are given in Table 1. With the exception of N23A, the mutants crystallize in monoclinic crystal forms with one tetramer in the asymmetric unit. The N23A mutant crystallizes with one monomer in the asymmetric unit in a tetragonal crystal form. All crystal forms adopted by these mutants had been observed previously for unbound or ligand-bound streptavidin (Schmidt *et al.*, 1996; Freitag *et al.*, 1997).

2.3. Data measurement

Diffraction data for the mutants were collected using in-house and synchrotron facilities. Statistics for the data sets are summarized in Table 1. Diffraction data for the unbound N23A and N23E mutants were collected on a Siemens–Nicolet–Xentronics area-detector system (Huber goniostat, Rigaku RU-200 rotating-anode X-ray source) at room temperature. The data sets for Y43A, both in the unbound state and in its complex with 2-iminobiotin, were collected using an R-AXIS II image-plate detector system (Rigaku RU-200 rotating-anode X-ray generator) at room tempera-

Table 1
X-ray data.

Values in parentheses are for the high-resolution shell.

Protein	N23A	N23A + biotin	N23E	S27A	S27A + biotin	Y43A	Y43A + 2-ib†	Y43F‡	Y43F + biotin
Space group	$I4_122$	$P2_1$	$P2_1$	$P2_1$	$P2_1$	$P2_1$	$P2_1$	$P2_1$	$P2_1$
Unit-cell parameters									
a (Å)	59.2	52.2	58.4	58.2	58.4	58.3	58.4	58.2	51.3
b (Å)	59.2	97.2	87.0	83.2	63.2	87.7	87.3	84.9	98.4
c (Å)	179.8	51.6	46.7	47.6	74.8	46.8	47.1	46.5	52.8
β (°)	90	112.6	98.9	98.7	92.8	98.9	99.0	98.8	112.9
Resolution (Å)	2.2	1.9	1.9	1.5	1.6	1.7	1.8	1.14	1.8
Unique reflections	8077	27213	27382	45399	55581	43769	34344	627749	35211
Completeness (%)	86 (62)	71 (43)	80 (33)	63 (0.3)	68 (0.1)	86 (35)	79 (28)	92 (81)	80 (30)
R_{merge}§¶	0.07 (0.25)	0.07 (0.25)	0.06 (0.33)	0.04 (—)	0.04 (—)	0.06 (0.41)	0.09 (0.79)	0.06 (0.14)	0.07 (0.32)
Data processing††	*SAINT*/*SADABS*	*DENZO*	*SAINT*/*SADABS*	*DENZO*	*DENZO*	*DENZO*	*DENZO*	*DENZO*	*DENZO*

† 2-Iminobiotin in subunit 1. ‡ Reported in Freitag *et al.* (1999). § On intensities. ¶ No entries for high-resolution shells containing no replicates. †† *DENZO* (Otwinowski & Minor, 1997), *SAINT*/*SADABS* (Siemens Industrial Automation Inc.).

Table 2
Refinement statistics.

Protein	N23A	N23A + biotin	N23E	S27A	S27A + biotin	Y43A	Y43A + ib†	Y43F‡	Y43F + biotin
Resolution range (Å)	10–2.2	10–1.9	10–1.9	10–1.5	10–1.6	10–1.7	10–1.8	10–1.14	10–1.8
Unique reflections	7392	27010	27129	45181	55319	43516	34086	149978	35008
Non-H atoms	912	3933	3621	4090	4168	3634	3523	3487	3790
Heteroatoms	—	64 (biotin)	—	40 (MPD)	64 (biotin)	8 (MPD)	16 (ib†)	48 (MPD)	64 (biotin)
Water molecules	63	360	175	400, 18 (0.5)§	459	151	101	373 (1.0), 177 (0.5)§	229
R factor¶	0.162	0.176	0.160	0.151	0.155	0.183	0.172	0.121	0.195
Free *R*¶††	0.212	0.275	0.252	0.235	0.203	0.245	0.235	0.151	0.274
R factor‡‡	0.187	0.195	0.186	0.157	0.159	0.211	0.201	0.126	0.227
Free *R*‡‡§§	0.253	0.301	0.284	0.243	0.248	0.273	0.266	0.157	0.312
Average *B* value (Å^2)									
Protein	29	22	30	19	20	34	35	15	24
Water	43	31	42	36	36	42	42	27	29
Heteroatoms	—	17	—	37	16	39	48	17	26
Ramachandran quality¶¶ (%)	99/81	97/78	99/89	98/81	99/81	98/82	98/82	99/82	97/78
R.m.s.d. (Å)									
Bond length	0.005	0.005	0.006	0.008	0.009	0.007	0.006	0.015	0.006
Bond angles	0.022	0.021	0.024	0.030	0.029	0.027	0.024	0.035	0.022
PDB code	1n4j	1n43	1n7y	1n9y	1n9m	1nbx	1n69	1swu	1ndj

† 2-Iminobiotin in subunit 1. ‡ Reported in Freitag *et al.* (1999). § O atoms of water molecules were refined with an occupancy of 1.0 unless the equivalent displacement parameter increased to over 0.5 Å^2. In cases of well defined water molecules with higher U_{eq} values, the occupancy was set to 0.5. ¶ For all data with $F > 4\sigma(F)$. †† For reflections in the test set§§ with $F > 4\sigma(F)$. ‡‡ For all data. §§ For 10% of the data. ¶¶ Fraction of residues in core regions/inner core regions (Kleywegt & Jones, 1996).

ture. The same device was used to collect data at 120 K for the biotin-bound form of N23A and the unbound and bound forms of S27A. The data sets for Y43F and Y43F–biotin were collected at 110 K at SSRL beamline 9-1. Data processing was carried out using the software cited in Table 1. Each data set was collected using one crystal.

2.4. Structure solution and refinement

All of the mutants discussed here are isomorphous with previously determined structures of streptavidin or its mutants and these models were used for initial phasing of the analyses described here. N23A was solved using a streptavidin–strep-tag peptide complex in the same crystal form (PDB code 1rst; Schmidt *et al.*, 1996). A ligand-free wild-type streptavidin model (PDB code 1swa; Freitag *et al.*, 1997) provided a starting point for the structures of the other unbound mutants (N23E, S27A, Y43A and Y43F). The initial model for the biotin-bound structures of N23A, Y43A and Y43F was a wild-type streptavidin–biotin complex (PDB code 1swe; Freitag *et al.*, 1997). The biotin-bound W79F structure (PDB code 1swk) was used for the first model of biotin-bound S27A. In all cases, only residues 16–44 and 53–132 of the search models were used for initial refinements. The flexible binding loop, solvent molecules and biotin were omitted from these initial models. (Crystals of biotin-bound N23E were also obtained, but the structure could not be solved.)

The structures were refined against squares of the structure-factor amplitudes (F^2) with the program *SHELXL*97 (Sheldrick & Schneider, 1997). The first refinement steps were full-matrix least-squares rigid-body refinements for the tetramer and for separate subunits. Conjugate-gradient least-squares methods were used and all parameters (coordinates and isotropic temperature factors) were refined together after the first rounds of refinement. 10% of the data were used for the calculation of R_{free} (Brünger, 1992), but were again included in the last refinement cycle. Distance, planarity and chiral volume restraints were applied, as were antibumping restraints. The target values for 1,2- and 1,3-distances were based on the Engh and Huber study (Engh & Huber, 1991). For the isotropic temperature factors, similarity restraints were applied. Diffuse solvent regions were modeled using Babinet's principle (Moews & Kretsinger, 1975). Anisotropic scaling of the observed structure factors (Parkin *et al.*, 1995) was applied for the refinements of Y43A and its 2-iminobiotin complex. Summary statistics for the refinements are presented in Table 2.

SHELXPRO was used for file formatting, model and data analyses and calculations of σ_A-weighted $|F_o| - |F_c|$ and $2|F_o| - |F_c|$ coefficients for electron-density maps (Read, 1986). The graphical evaluation of the model and electron-density maps was carried out with *XtalView* (McRee, 1999). The stereochemistry was checked during the refinement process with the programs *PROCHECK* (Laskowski *et al.*, 1993) and *WHAT IF* (Vriend & Sander, 1993). Most of the refined water positions were found by *SHELXWAT* and the geometry of each water molecule was checked interactively. Water O atoms were rejected when *B* values increased above 63 Å^2 (U = 0.8 Å^2). The H atoms were set to idealized positions and refined with a riding model. The coordinates of the mutant structures have been deposited in the PDB.

3. Results

All of the streptavidin mutants described here adopt the folding found for the wild-type protein (Hendrickson *et al.*, 1989; Weber *et al.*, 1989). For structural comparisons across different crystal forms, the bound and unbound proteins were

superposed onto the biotin-bound wild-type structure (PDB code 1swe) using 65 C^{α} atoms in the β-barrels of each subunit in the tetramer (residues 19–23, 28–33, 38–42, 54–60, 71–80, 85–97, 103–112 and 123–131).

3.1. N23A mutant

The N23A mutant crystallizes with only one monomer in the asymmetric unit. For comparisons with the wild-type structures, a whole tetramer with 222 symmetry was generated applying the crystallographic symmetry operations. Residues 16–133 were observed for the unliganded form, with the partial biotin-binding loops in the open conformation. The N23A–biotin complex structure is a tetramer (residues 16–133) with biotin in all four subunits and the binding loop closed over the ligand. Fig. 2 shows the structures of biotin-bound and unbound N23A superposed on the structure of biotin-bound wild-type streptavidin.

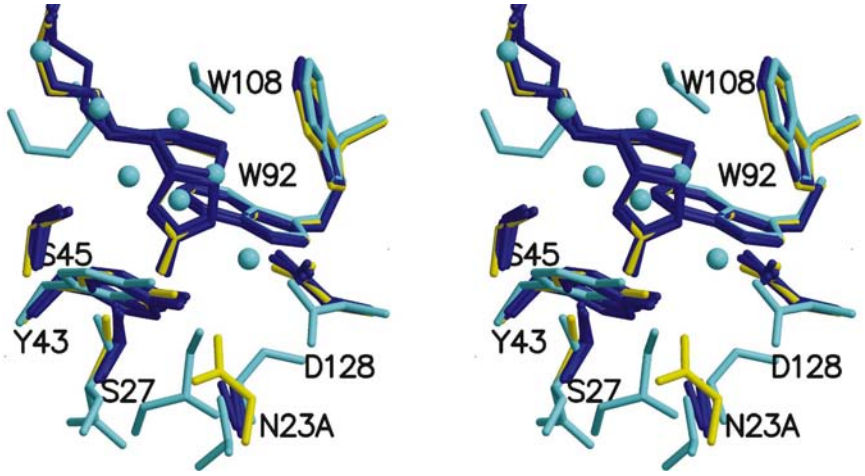

Figure 2
Stereoview of the structures of the N23A mutant superposed on the biotin complex of wild-type streptavidin. The biotin-bound structure of N23A is shown in dark blue, the unbound structure is in light blue and the wild-type structure is in yellow. Figure drawn with *MOLSCRIPT* (Kraulis, 1991) and *Raster3D* (Merritt & Bacon, 1997).

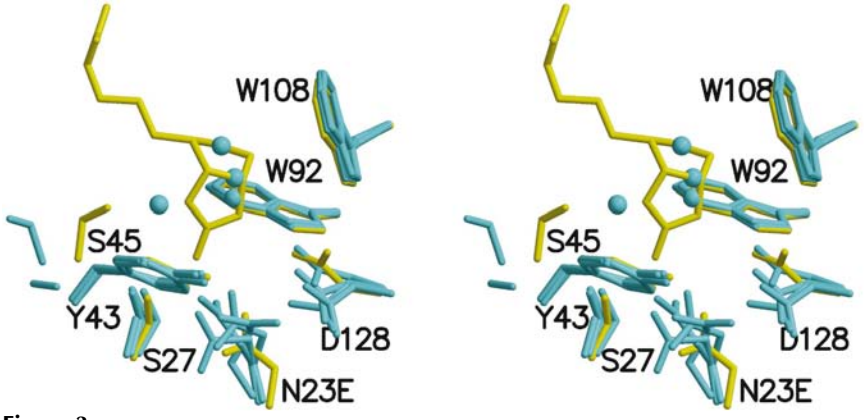

Figure 3
Stereoview of the superposition of N23E on wild-type streptavidin. The four subunits of unbound N23E in the asymmetric unit are shown in light blue. Biotin-bound wild-type streptavidin is in yellow. Figure drawn with *MOLSCRIPT* (Kraulis, 1991) and *Raster3D* (Merritt & Bacon, 1997).

The shorter side chain introduced into the N23A mutant is associated with local structural changes and not extensive alterations in loop conformations or overall molecular dynamics. Introduction of the mutation does not significantly affect the thermal parameters for any portion of the protein.

A small change in the unbound N23A structure involves the side chain of Asp128, which is shifted from its position in wild-type streptavidin. In addition to the cavity formed by the N23A mutation, the side chain of Glu24 moves from its wild-type position to become more solvent-exposed. The side chain of Asp128 shifts to occupy part of the space formerly filled by Glu24 and a water molecule is then bound where the carboxylate of residue 128 used to be. This additional water molecule is 2.6 Å from the nearest water site in the unbound wild-type structure.

In the bound structure, Asp128 retains its wild-type position and makes a hydrogen bond with the N2 atom of biotin. In this structure, a void is left when the mutated Asn23 is shortened to alanine. There should be sufficient volume for a water molecule to occupy this space, but no electron density for one is observed.

3.2. N23E mutant

The four monomers in the unbound N23E structure show small conformational changes at the site of mutation and at residue 128. The side chain of the glutamic acid itself shows conformational variability (Fig. 3) when the four monomers are superposed onto biotin-bound wild-type streptavidin. Lengthening the side chain by one methylene group increases its solvent exposure and the molecule rearranges its structure to minimize these effects. No single side-chain conformer is found in the four subunits in the asymmetric unit, nor is a single response of Asp128 found. In the monomer where Asp128 moves the furthest, a water molecule moves in to substitute for it in the network of water–protein hydrogen bonds and to fill the space created by the mutation.

3.3. S27A mutant

In the unbound S27A mutant, the side chain of Asp128 again shows different conformations in the four monomers (Fig. 4). In the conformation that is farthest away from that in the biotin complex, a water molecule is found forming a hydrogen bond between an MPD molecule in the biotin-binding site and OD1 and OD2 of Asp128.

In the structure of S27A with biotin bound to the protein, a water molecule replaces the OG1 of the serine and makes a

hydrogen bond (2.95 Å) with the ureido oxygen of biotin. This serves as a replacement for the hydrogen-bonding partner lost in the mutation. Asp128 does not show different conformations in the four monomers when biotin is present. It remains a hydrogen-bonding partner for N2 of biotin. Even with a hydrogen-bonding partner replaced by a water molecule, the biotin affinity of the mutant is still lower than for wild-type protein (ΔK_d = 114), but is not as low as in N23A where no water fills the newly formed cavity.

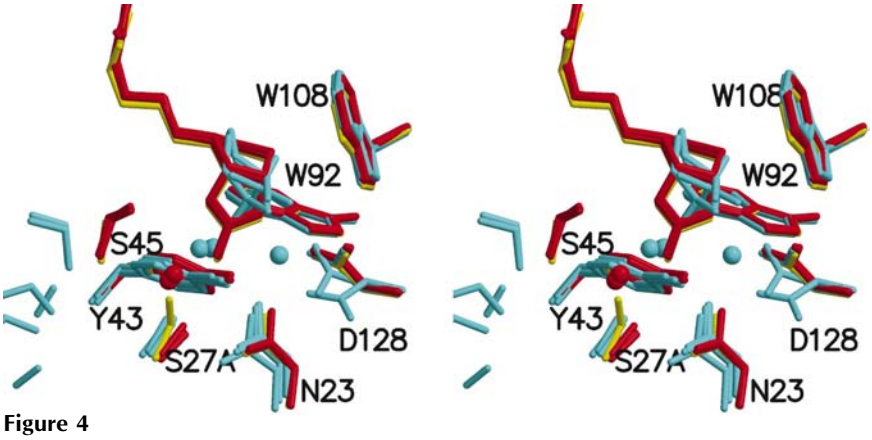

Figure 4
Stereoview of the superposition of S27A on wild-type streptavidin. The four independent subunits in the unbound S27A structure are shown in light blue. The biotin-bound complex of S27A is shown in red. Wild-type streptavidin is shown in yellow. Figure drawn with *MOLSCRIPT* (Kraulis, 1991) and *Raster3D* (Merritt & Bacon, 1997).

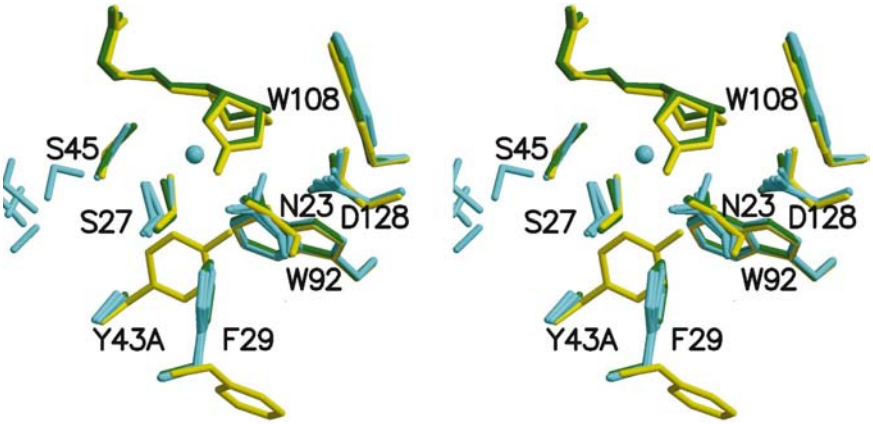

Figure 5
Stereoview of the superposition of Y43A on wild-type streptavidin. Unbound Y43A is in light blue. The imidobiotin complex of Y43A is in green. Wild-type streptavidin is in yellow. Figure drawn with *MOLSCRIPT* (Kraulis, 1991) and *Raster3D* (Merritt & Bacon, 1997).

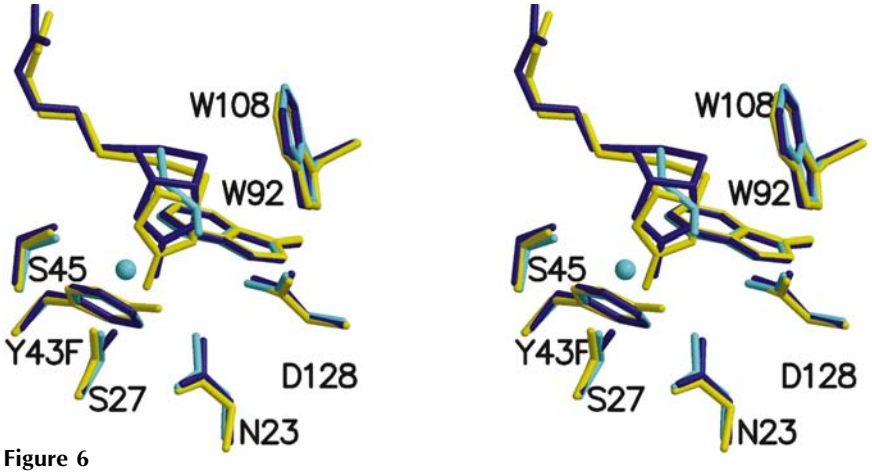

Figure 6
Stereoview of the superposition of Y43F on wild-type streptavidin. Unbound Y43F in light blue, bound Y43F in dark blue and wild-type streptavidin in yellow. The binding site in the unbound Y43F structure is occupied by a water molecule and an MPD molecule (Freitag *et al.*, 1999). Figure drawn with *MOLSCRIPT* (Kraulis, 1991) and *Raster3D* (Merritt & Bacon, 1997).

3.4. Y43A mutant

In the unbound Y43A mutant, the neighboring Phe29 aromatic side chain shifts towards the void created by the mutation (Fig. 5). This shift is an almost 180° rotation of χ_1 for Phe29. It is observed in all monomers of the unbound protein. Two other residues display small systematic shifts connected to the change in Phe29. The side chain of Trp75 in the Y43A mutant is tilted toward the former Phe29 side-chain position and the Phe130 phenyl ring also shifts toward this position. It is interesting that all involved residues have aromatic side chains which are able to interact *via* hydrophobic interactions, but are on the other hand also sterically restrained.

3.5. Y43F mutant

The structure of unbound Y43F streptavidin has been described previously (Freitag *et al.*, 1999). The atomic resolution of the Y43F structure (1.14 Å) made it possible to refine disordered side chains, anisotropic displacement parameters and a more accurate water model. In addition, 2-methyl-2,4-pentanediol (MPD) from the crystallization solution was detected in the biotin-binding site for the first time.

Only minor deviations from the wild-type streptavidin structures are observed for the unbound and bound structures of Y43F (Fig. 6). The largest structural difference observed is the loss of the phenol hydroxyl group on residue 43. These minor changes agree very well with the thermodynamic and kinetic data, where Y43F has the smallest change in affinity, with a ΔK_d of 7.

4. Discussion and conclusions

The streptavidin mutants studied here were designed to probe the energetic contributions of hydrogen-bonding groups that interact with the ureido oxygen of biotin. The equilibrium and activation thermo-

Table 3
Summary of kinetic and thermodynamic data for streptavidin mutants at 310 K.

Taken from Klumb *et al.* (1998).

	k_{off} (10^{-5} s^{-1})	Δk_{off}†	ΔK_d§	$\Delta\Delta G^\circ$¶ (kJ mol^{-1})	ΔH° (kJ mol^{-1})	$\Delta H^\ddagger$ (kJ mol^{-1})	$T\Delta S^\ddagger$ (kJ mol^{-1}) (310 K)	$\Delta G^\ddagger$ (kJ mol^{-1}) (310 K)
Wild type	4.3 ± 0.2		0.96 ± 0.04		−123	127 ± 0.8	24.2 ± 0.4	103 ± 1.3
N23A	1030 ± 220	251	282 ± 9	14.6	−90	93 ± 1.7	5.9 ± 1.7	87 ± 2.5
N23E	770 ± 60	188	69 ± 3	2.6	−107	84 ± 2.1	−5.4 ± 2.1	89 ± 2.5
S27A	660 ± 40	161	114 ± 3	10.9	−102	108 ± 1.3	19 ± 1.3	89 ± 1.7
Y43A	380 ± 60	93	67 ± 3	10.9	−90	94 ± 2.1	2.5 ± 2.1	91 ± 2.9
Y43F	20 ± 1	4.9	6.9 ± 0.2	5.0	−118	131 ± 1.3	32.2 ± 0.8	98 ± 1.3

† $\Delta k_{off} = k_{off}$(mutant)/k_{off}(wild type). § $\Delta K_d = K_d$(mutant)/K_d(wild type). ¶ $\Delta\Delta G^\circ = \Delta G^\circ$(mutant) − ΔG°(wild type) = $RT\ln\Delta K_d$.

Table 4
Average hydrogen-bond lengths (Å) in wild-type and mutant streptavidin–biotin (2-iminobiotin) complexes.

Values in parentheses are the r.m.s. deviation from the mean for the observations for each mutant.

Biotin† atom	Protein atom	Wild-type	N23A	S27A	Y43A†	Y43F
O3 (N3†)	Asn23 ND2	3.05(0.05)	—	3.16 (0.07)	2.78	2.85 (0.08)
O3 (N3†)	Ser27 OG	2.63 (0.14)	2.42 (0.08)	—	3.09	2.48 (0.17)
O3 (N3†)	Tyr43 OH	2.74 (0.10)	2.57 (0.09)	2.88 (0.05)	—	—
O1	Asn49 N	2.80 (0.18)	2.80 (0.06)	2.98 (0.08)	2.68	2.98
O2	Ser88 OG	2.86 (0.21)	2.79 (0.21)	2.93 (0.04)	3.09	2.89 (0.14)
S1	Thr90 OG1	3.37 (0.08)	3.28 (0.08)	3.43 (0.05)	3.29	3.20 (0.15)
N1	Ser45 OG	3.10 (0.10)	3.01 (0.18)	3.19 (0.03)	2.95	3.09 (0.26)
N2	Asp128 OD2	2.76 (0.07)	2.74 (0.06)	2.93 (0.07)	3.00	2.86 (0.16)

† 2-Iminobiotin for Y43A only in subunit 1, so no r.m.s. deviations can be calculated.

dynamic alterations associated with these site-directed mutants are summarized for reference in Table 3. The thermodynamic analyses raised three key questions connected to structure: (i) were there any significant structural alterations induced by mutation, (ii) were there detectable changes in the presence or absence of water and (iii) could structural changes and water alterations provide insight into the observed energetic alterations? We consider each of these questions in turn here.

Superposition of the four biotin-bound mutant structures on the biotin-bound wild-type protein shows that the position of biotin in the binding pocket is not significantly altered by mutation (Fig. 7, Table 4). Similarly, there were no significant alterations in side-chain positions in any of the biotin-bound structures for the conservative mutations N23A, S27A and Y43F. The bound structures for Y43A and N23E were not obtained, although the iminobiotin complex for Y43A was determined and no significant side-chain alterations were observed. While the bound structures were highly conserved, there were significant structural alterations observed in the unbound structures. The largest side-chain alteration observed was found in the Y43A structure, where the neighboring Phe29 side chain undergoes a large χ_1 rotation to fill the space formerly occupied by the missing phenolic moiety. This new position for the Phe29 side chain is also seen in the iminobiotin complex. There is also a significant structural alteration in the unbound N23A mutant. The adjacent Asp128 side chain moves toward the position of the missing side-chain amide atoms and an ordered water molecule is found at the old position of the carboxylate O atoms.

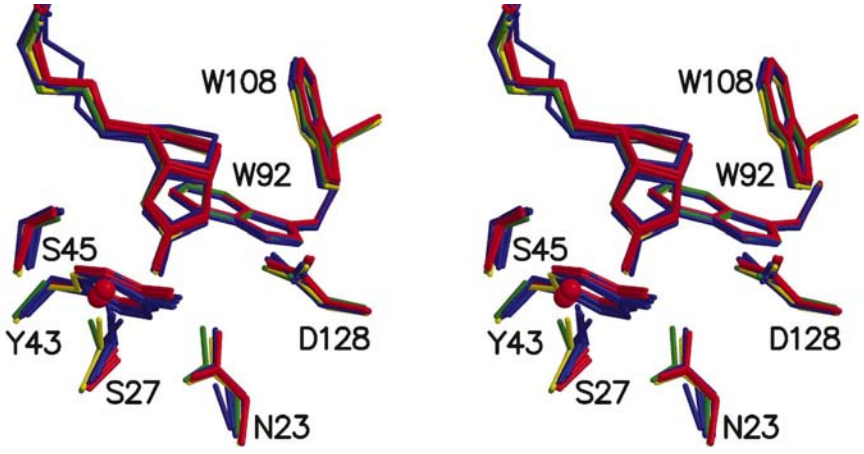

Figure 7
Stereoview of the superposition of biotin and imidobiotin complexes on wild-type streptavidin. N23A in blue, S27A in red, Y43A in green, Y43F in dark blue, wild-type in yellow. Figure drawn with *MOLSCRIPT* (Kraulis, 1991) and *Raster3D* (Merritt & Bacon, 1997).

An important question with these structures was whether water molecules moved in to replace the missing hydrogen-bonding donor atoms that were removed by mutation. In the bound structures, only the S27A mutation resulted in an ordered water molecule moving into the position of the missing side-chain atoms. The new water

molecule was positioned nearly identically to the missing OG1 atom and within tight hydrogen-bonding distance of the ureido oxygen of biotin. Neither the N23A nor Y43F mutants were observed to contain a new water molecule to fill the void left by the missing hydrogen-bonding donors.

These structures provide important new information that is relevant to the previous energetic analysis. The Y43F mutant displayed a binding enthalpy that was surprisingly more negative than the wild type, but the corresponding unfavorable change in the entropy term led to an overall decrease in binding free energy. We had noted the similarity of this signature to a previous mutagenesis study of a Tyr→Phe alteration in FK506, where a water molecule was suggested to account for this type of alteration in the enthalpy/entropy signature (Pearlman & Connelly, 1995). Specifically, the decrease in entropy was interpreted in terms of a decrease in entropy associated with water release from the phenyl side chain compared with release of two water molecules hydrogen bonded to the phenolic side chain.

The observation that a water molecule replaces the missing O atom and hydrogen-bonding interaction in the S27A mutant could explain the relatively small 6.7 kJ mol^{-1} $\Delta\Delta H^0$ (299 K) alteration in the binding enthalpy relative to wild-type streptavidin. The corresponding $\Delta\Delta H^0$ for N23A was 28.9 kJ mol^{-1}, with a correspondingly large and only partly compensating $T\Delta S^0$ term (again at 298 K). The ordering of this water molecule in the bound S27A complex could also play a significant role in the 5.4 kJ mol^{-1} increase in the unfavorable entropy term associated with biotin binding. In the S27A mutant, the overall decrease in binding enthalpy arises from both a reduction in binding enthalpy and a less favorable entropy term, while the N23A decreasearises from a large reduction in binding enthalpy that is actually significantly offset by a more favorable entropy term. The involvement of a water molecule in the S27A–biotin complex and its absence in the N23A complex is consistent with these differences in their thermodynamic signatures.

This work was supported by grant DK49655 from the National Institutes of Health. We thank the Murdock Foundation for financial support in the Biomolecular Structure Center. Portions of this research were carried out at the Stanford Synchrotron Radiation Laboratory, a national user facility operated by Stanford University on behalf of the US Department of Energy, Office of Basic Energy Sciences. The SSRL Structural Molecular Biology Program is supported by the Department of Energy, Office of Biological and Environmental Research and by the National Institutes of Health, National Center for Research Resources, Biomedical Technology Program and the National Institute of General Medical Sciences.

References

Brünger, A. T. (1992). *Nature (London)*, **355**, 472–475.
Chilkoti, A. & Stayton, P. S. (1995). *J. Am. Chem. Soc.* **117**, 10622–10628.
Chilkoti, A., Tan, P. H. & Stayton, P. S. (1995). *Proc. Natl Acad. Sci. USA*, **92**, 1754–1758.
Chu, V., Freitag, S., Le Trong, I., Stenkamp, R. E. & Stayton, P. S. (1998). *Protein Sci.* **7**, 848–859.
Engh, R. A. & Huber, R. (1991). *Acta Cryst.* A**47**, 392–400.
Freitag, S., Le Trong, I., Chilkoti, A., Klumb, L. A., Stayton, P. S. & Stenkamp, R. E. (1998). *J. Mol. Biol.* **279**, 211–221.
Freitag, S., Le Trong, I., Klumb, L., Stayton, P. S. & Stenkamp, R. E. (1997). *Protein Sci.* **6**, 1157–1166.
Freitag, S., Le Trong, I., Klumb, L. A., Stayton, P. S. & Stenkamp, R. E. (1999). *Acta Cryst.* D**55**, 1118–1126.
Green, N. M. (1963). *Biochem. J.* **89**, 599–609.
Hendrickson, W. A., Pahler, A., Smith, J. L., Satow, Y., Merritt, E. A. & Phizackerley, R. P. (1989). *Proc. Natl Acad. Sci. USA*, **86**, 2190–2194.
Hyre, D. E., Le Trong, I., Freitag, S., Stenkamp, R. E. & Stayton, P. S. (2000). *Protein Sci.* **9**, 878–885.
Kleywegt, G. J. & Jones, T. A. (1996). *Structure*, **4**, 1395–1400.
Klumb, L. A., Chu, V. & Stayton, P. S. (1998). *Biochemistry*, **37**, 7657–7663.
Kraulis, P. J. (1991). *J. Appl. Cryst.* **24**, 946–950.
Laskowski, R. A., MacArthur, M. W., Moss, D. S. & Thornton, J. M. (1993). *J. Appl. Cryst.* **26**, 283–291.
McRee, D. E. (1999). *J. Struct. Biol.* **125**, 156–165.
Merritt, E. A. & Bacon, D. J. (1997). *Methods Enzymol.* **277**, 505–524.
Moews, P. C. & Kretsinger, R. H. (1975). *J. Mol. Biol.* **91**, 201–228.
Otwinowski, Z. & Minor, W. (1997). *Methods Enzymol.* **276**, 307–326.
Parkin, S., Moezzi, B. & Hope, H. (1995). *J. Appl. Cryst.* **28**, 53–56.
Pearlman, D. A. & Connelly, P. R. (1995). *J. Mol. Biol.* **248**, 696–717.
Read, R. J. (1986). *Acta Cryst.* A**42**, 140–149.
Schmidt, T. G., Koepke, J., Frank, R. & Skerra, A. (1996). *J. Mol. Biol.* **255**, 753–766.
Sheldrick, G. M. & Schneider, T. R. (1997). *Methods Enzymol.* **277**, 319–343.
Vriend, G. & Sander, C. (1993). *J. Appl. Cryst.* **26**, 47–60.
Weber, P. C., Ohlendorf, D. H., Wendoloski, J. J. & Salemme, F. R. (1989). *Science*, **243**, 85–88.